

SIMULATION OF SURFACE IRRIGATION SYSTEM USING EXPLICIT FINITE DIFFERENCE METHOD

Mrugen Dholakia¹

Rajeev Misra²

ABSTRACT

A hydrodynamic model for simulating the flow in Basin irrigation system is presented. An explicit McCormack method is used for solving the governing equations. This method doesn't require any special treatment of advancing or receding fronts such as sub-grid technique. The numerical procedure accommodates for three inflow boundary conditions namely line inflow, corner inflow and fan inflow. The results are compared with observed advance and recession times for two level basin irrigation events available in the literature and two field experiments conducted by authors at WALMI, Vadod, Anand, Gujarat, India. A very good comparison of results is observed. The results for various other cases are also presented.

INTRODUCTION

Basin irrigation is the most popular method of irrigation in India. The effective and optimal utilization of water through basin irrigation system has drawn attention of irrigation as well as agricultural engineers. Conventionally, the Indian basins are level as well as graded, having considerable slope in both the directions and a low length to width ratio. Hence, the flow over both level and graded basins is two-dimensional, spatially varied and unsteady. Several mathematical models have been developed to numerically integrate the two-dimensional unsteady flow equations in open channels for various applications such as dam breach flood (*Xanthopoulos and*

-
1. Asst. Prof., Dept. of Civil Engineering, L. D. College of Engineering, Ahmedabad 380 015, Gujarat, India.
 2. Asst. Prof., Dept. of Civil Engineering, Indian Institute of Technology, Bombay, Powai, Mumbai, 400 076, India.

Kautitas 1976, Katopodes and Strelkoff 1978), tidal flow in estuaries (Walter and Cheng 1979, Mader 1988, Casulli 1990), discontinuous and supercritical flows (Katopodes 1980 and Katopodes and Wu 1986), channel transitions (Chaudhry 1993), etc. These models numerically integrate the flow equations using method of characteristics (Katopodes and Strelkoff 1978), finite difference (Mader 1988, Casulli 1990, Reid and Bodine 1968, Chaudhry 1993) and finite element methods (Katopodes 1980, Walters and Cheng 1979, Katopodes and Wu 1986, Akanbi and Katopodes 1988).

The application of numerical techniques to simulation of flow in basin irrigation systems is very limited. Akanbi and Katopodes (1988) used their finite element technique in a model for two-dimensional overland flow. Playan et al. (1994) used a variation of Leap-Frog finite difference scheme for basin irrigation system. These two existing models simulate for flow over the surface during the advance phase only. Once the advance is reached, the simulation is stopped and the surface flow depths are allowed to recede. The simulation of flow during the ponding and recession phase is not performed. These modelling simplifications result, in significant errors especially in case of graded basins. Singh and Murthy (1998) presented a hydrodynamic model for level basins. They suggested the use of sub-grid technique to improve the accuracy.

The paper presents a computational model developed to simulate the flow in a basin irrigation system. The applicability of McCormack finite difference method to basin irrigation system is demonstrated. The governing differential equations of dynamic wave are solved using explicit McCormack the method. The initial experience with the model suggests that the implementation of the boundary conditions is very important especially while simulating the depletion and recession phase in basin irrigation. Three types of inflow boundary conditions are implemented in the model corresponding to three irrigation practices (Playan et al. 1994). The capability of the models to deal with internal high spots, point or linear inlet and the flow over an irrigation field with spatially varied infiltration characteristics is demonstrated. The results of the models are compared with the field measured advance and recession times for two sets of data on level basin (Playan et al. 1994). An excellent agreement of results

with the field observations is obtained. The model is also used to simulate flow in basin at WALMI, Vadod, Gujarat, India. The simulation results are compared with field experiments conducted by authors.

FORMULATION

The general form of governing equations for two-dimensional flow over the basin irrigation system can be concisely written as,

$$\frac{\partial U}{\partial t} + \frac{\partial E}{\partial x} + \frac{\partial F}{\partial y} + S = 0 \quad (1)$$

Where, x, y = distances along either of the sides of the basin, t = time.

For complete hydrodynamic equations for basin irrigation systems (Playan et al. 1994),

$$U = \begin{bmatrix} h \\ q_x \\ q_y \end{bmatrix} \quad E = \begin{bmatrix} q_x \\ \frac{q_x^2}{h} + \frac{gh^2}{2} \\ \frac{q_x q_y}{h} \end{bmatrix} \quad F = \begin{bmatrix} q_y \\ \frac{q_x q_y}{h} \\ \frac{q_y^2}{h} + \frac{gh^2}{2} \end{bmatrix} \quad S = \begin{bmatrix} I \\ -gh(S_{ox} - S_{nx}) + \frac{q_x}{h} \left(\frac{I}{2}\right) \\ -gh(S_{oy} - S_{ny}) + \frac{q_y}{h} \left(\frac{I}{2}\right) \end{bmatrix} \quad (2)$$

Where q_x = unit discharge in the x -direction (m^2/s), q_y = unit discharge in y -direction (m^2/s), h = flow depth (m), g = acceleration due to gravity (m/s^2) and n =

Manning's roughness coefficient; $S_{fx} = g n^2 \frac{q_x (q_x^2 + q_y^2)^{1/2}}{h^{10/3}}$;

$S_{fy} = g n^2 \frac{q_y (q_x^2 + q_y^2)^{1/2}}{h^{10/3}}$; I = infiltration rate and can be computed from Kostiakov-Lewis equation (Playan et al. 1994).

$$I = abt^{b-1} + c \quad (3)$$

Where τ = opportunity time (min), b = exponent and c = a coefficient (m/min). The time-integrated form of Eq. 3 provides the expression for the infiltrated depth,

$$z = a\tau^b + c\tau \quad (4)$$

COMPUTATIONAL METHOD

Fig. 1 shows the finite-difference discretization of the domain in two dimensions. Using McCormack finite difference approximation, Eq. 1 can be written as,

Predictor Step

$$U_{i,j}^{k*} = U_{i,j}^k - \frac{\Delta t}{\Delta x} (E_{i+1,j}^k - E_{i,j}^k) - \frac{\Delta t}{\Delta y} (F_{i,j+1}^k - F_{i,j}^k) - \Delta t (S_{i,j}^k) \quad (5)$$

Corrector step

$$U_{i,j}^{k**} = U_{i,j}^{k*} - \frac{\Delta t}{\Delta x} (E_{i+1,j}^{k*} - E_{i,j}^{k*}) - \frac{\Delta t}{\Delta y} (F_{i,j+1}^{k*} - F_{i,j}^{k*}) - \Delta t (S_{i,j}^{k*}) \quad (6)$$

The value of the variable at the new time level is,

$$U_{i,j}^{k+1} = 0.5 (U_{i,j}^k + U_{i,j}^{k**}) \quad (7)$$

The details of this procedure for solving the hydrodynamic equations are available in standard text in open channels (Chaudhry 1993).

INITIAL CONDITION

Zero depth and discharge should be taken as initial condition. However, to avoid undefined terms resulting due to mathematical singularity at the beginning of the computation, a small positive value of 10^{-10} m is initially assigned to the depth of flow at all

computational nodes in the domain. The same value is used to initialize q_x and q_y .

BOUNDARY CONDITIONS

The simulation of basin irrigation system requires the implementation of proper inflow boundary conditions. The numerical method used is applicable at all interior nodes only and special treatment is required for evaluating ' q_x ', ' q_y ' and ' h ' at the boundary nodes. Three types of inflow boundary conditions are implemented in the model. These correspond to three irrigation practices namely line inflow, corner inflow and fan inflow. A description of each type is given by *Playan et al. (1994)*. For the line inflow the boundaries involved are the flow boundaries and the symmetry boundaries. A flow boundary can be either an inflow boundary or an outflow boundary. Pseudo boundary nodes are adopted to determine the boundary conditions especially if an explicit scheme is used (*Dholakia 1998*). A reflection procedure is used at a symmetry boundary (*Roache 1972*).

ADVANCE PHASE, RECESSON PHASE AND INFILTRATION

A procedure adopted by *Playan et al. 1994* is used to define the advance phenomenon by ignoring all flow depths smaller than a certain user-defined threshold (the minimum flow depth needed for the node to be considered as part of advancing front and that which allows infiltration to start). This minimum depth must be greater than the initial depth. Values equal to/or smaller than 10^{-3} m did not modify the advance rate of quasi-one-dimensional simulations (*Playan et al. 1994*). The end of advance phase occurs when flow depth at all nodes in the domain is greater than the minimum threshold infiltration depth (10^{-3} m). The value of the time at this point is the time of advance. Similarly, the recession phase, thereby end of simulation occurs when the flow depth at all nodes in the domain is less than minimum threshold value.

STABILITY

Explicit finite difference schemes are stable as long as the *Courant-Friedrichs-Lewy (CFL)* condition is satisfied. For two-dimensional flows it is expressed as,

$$C_{2d} = \left(\frac{|V| + \sqrt{gh}}{\Delta x \Delta y} \right) \Delta t \sqrt{\Delta x^2 + \Delta y^2} \leq 1 \quad (8)$$

Where, 'V' is the resultant velocity at the grid point. Eq. 8 has to be satisfied at every grid point at all times

VALIDATION AND COMPARISON OF MODELS

The computational model is developed to simulate the flow in level as well as graded basins. A comparison of this model with B2D and SIRMOD (*Playan et al. 1994*) is presented.

Line inflow

A narrow rectangular level basin is used to simulate the model in quasi-one-dimensional conditions (*Playan et al. 1994*). The basin was 465 m long and 100-m wide, with an area of 46,500-m² and was irrigated from one of its 100-m sides. Water flowing in this field experiment was largely one-dimensional. The field had no significant slope. The infiltration parameters obtained were, $a = 0.00893 \text{ m/min}^b$, $b = 0.406$ and $c = 0.00000 \text{ m/min}$. A value of 0.1 was estimated for the Manning's 'n'. The field was irrigated with a constant discharge of 0.183 m³/sec, measured with a broad-crested weir. The inflow was cut-off after 660 min. A quasi-one-dimensional simulation is performed using hydrodynamic model. A line inflow is defined along one of the 100-m sides of the basin and the grid spacing was set to 5-m.

Fig. 3 presents the advance profiles at times 180, 360 and 540 minutes simulated by SIRMOD, B2D and proposed hydrodynamic model BASIIT. Table 1 presents the advance and recession times for the field

data as obtained by SIRMOD, B2D and BASIIT. Both SIRMOD and B2D underestimated the time of advance. B2D underestimated the advance by 5.5 % and SIRMOD underestimated by 3.6 %. Whereas, BASIIT underestimated the advance by 4.0 %. All the models produced a straight horizontal recession line because the field slopes were set to zero. B2D overestimated the average recession time by 0.4 %, while SIRMOD underestimated by 4.4 %. BASIIT overestimated estimated the recession time by 0.8 %.

Corner inflow

To test the two-dimensional predictive capability of the model, 216.1-m long by 183.2-m wide field having an area of 39,590-m² is used (Playan et. al. 1994). The infiltration parameters were determined by means of three dual ring cylinder infiltrometer tests as, $a = 0.0168$ m/min^b; $b = 0.397$ and $c = 0.0$ m/min. A value of 0.10 was estimated for the Manning roughness coefficient 'n'. The field was irrigated from its northwest corner with a constant discharge of 0.270 m³/sec. The inflow was cut-off after 540 minutes. Field observed response is compared with results obtained by SIRMOD, B2D, and BASSIF model. A 21 by 21 grid is used in the models to represent the domain and the field is simulated as a corner inflow.

Figs. 4, 5, 6, 7 present the front configuration for corner inflow at 3h, 5h, 6h and 7h simulated by finite difference models BASIIT. The results obtained by B2D and SIRMOD are also presented in these figures. Table 1 also presents the advance and recession times as obtained by SIRMOD, B2D, and BASIIT. Both SIRMOD and B2D underestimated the time of advance. B2D underestimated the advance by 7.9 % and SIRMOD underestimated by 17.5 %. Whereas, BASIIT underestimated the advance by 8.0 %. B2D underestimated the average recession time by 0.4 %, while SIRMOD it underestimated by 15.4 %. Whereas, BASIIT underestimated the recession time by 0.78 %.

Fronts simulated by all the models are symmetrical for the second and third hour, while the corresponding fronts for field data show faster advance in the southern direction (Figs. 4-7). This seems to be due to the configuration of the inlet, microtopography and spatially varied infiltration. After the third hourly

profile, the advancing front reaches the domain's southwest corner and the front configuration loses symmetry, but the effect of preferential flow towards the south is still noticeable in the field data. SIRMOD can only predict the front configuration as a straight line, while B2D and BASIIT approximate the front configurations.

The simulated advance by BASIIT compare excellently with the observed advance of level basins. Similarly, the simulated recession of the model compare satisfactorily. The results suggest that the explicit model can simulate the complete irrigation event with a fair degree of precision.

MODEL APPLICATION

High spots

A hypothetical case study is used to illustrate the additional feature of the model namely its capability to include high spots (Islands) inside the domain. A domain is sketched over rectangular grid composed of 21 rows and 29 columns, with a uniform grid spacing of 5m. An internal high spot is considered within the domain. A line inflow is distributed along north side of the domain, with a discharge of $0.250 \text{ m}^3/\text{s}$ and a cut time of 50.0 min. The infiltration parameters are, $a = 0.00346 \text{ m}/\text{min}^b$, $b = 0.388$ and $c = 0.000057 \text{ m}/\text{min}$ (Playan et al. 1994). Fig. 8 presents the overland water surfaces for times 30 minutes. The flow circumvents the high spot and both the flow branches meet on the downstream side.

A second hypothetical case study is considered to illustrate the flow past the high spot using corner inflow configuration. A corner inflow is distributed along a square field 100 m long, with a discharge of $0.1 \text{ m}^3/\text{sec}$. The inflow is cut-off after 60 min. Manning's 'n' is 0.04, and the infiltration parameters are $a = 0.00323 \text{ m}/\text{min}^b$, $b = 0.474$ and $c = 0.000098 \text{ m}/\text{min}$ (Playan et al. 1994). Fig. 9 presents the overland water surfaces for time 40 minutes. In this case also the flow circumvents the high spot and both the flow branches meet on the downstream side.

Fan inflow

BASIIT is used to simulate the flow in a hypothetical square field 50 m long, with an area of 2500 sq. m., irrigated with a constant discharge of 0.05 m³/sec using a fan inflow configuration. The inflow is cut-off after 30 min. Manning's 'n' is 0.04 and the infiltration parameters are, a = 0.00323 m/min^b, b = 0.474 and c = 0.000098 m/min. Different node configurations are used to represent field, ranging from 121 to 676 nodes domain. Table 2 presents the results of this test for the fan inflow. In this inflow configuration, Δt decreases as the grid becomes finer due to the effect of Δx and Δy . Flow depth and velocity are locally increased resulting in shorter time steps. Between 121 node and 676-node configuration, the variation in advance time is 12 % and in recession time is 1.6 %. The mass balance errors varied from 0.456 % to 0.683 %. Fig. 10 presents the overland profiles during the advance at 15 minutes.

Spatially varied infiltration

It is a common practice to conduct tests at several locations within each field to account for the effects of spatial variability. The parameters are then estimated statistically fitting a curve to the data pairs resulting from all the tests. The result is an averaged infiltration curve that represents the whole field.

The infiltration rate at any point 'p' in the field with an opportunity time ' τ_p ' can be interpolated using an inverse distance square procedure (Playan et al. 1994),

$$i_p = \frac{\sum_{j=1}^m b_j a_j \tau^{b_j-1} + c_j}{\sum_{j=1}^m \frac{1}{d_{pj}^2}} \quad (9)$$

Where m = number of test sites, a_j , b_j and c_j = infiltration parameters corresponding to test site j; and d_{pj} = distance between the point p and the test site j (m).

BASIIT interpolates the value of the infiltration rate for each node in the finite-differencing grid and uses it to solve the governing equations for the dependent variables. The infiltrated depth at each node is then computed using the following expression,

$$z_p^{t+\Delta t} = z_p^t + i_p^{t+\Delta t} \Delta t \quad (10)$$

The model is applied to a hypothetical square field with an area of 10,000-m². The inflow discharge is 0.100 m³/s with an application time of 100 min. Only corner inflow cases were considered in this study. Five case studies are considered in the analysis of the problem. Case studies NWC, NEC, SWC and SEC correspond to water sources located in the Northwest, Northeast, Southeast, and Southwest corners, respectively. All of them implement spatially varied infiltration. Finally, the UNI case study corresponds to a uniform infiltration analysis of the problem, where the field is irrigated from the Northeast corner (Fig. 11) and infiltration is characterised by a statistical regression of the five test sites, which gives average values of, $a = 0.00264 \text{ m/min}^b$, $b = 0.639$ and $c = 0.000025 \text{ m/min}$.

Simulation results for all five cases are presented in Table 3. It compares the time of advance (T_a), time of recession (T_r), required depth (z_r), application efficiency (E_a), water requirement efficiency (E_r) and distribution uniformity of low quarter (D_u) for the different cases. Figs. 12 and 13 presents three-dimensional maps of infiltrated depth for case NEC and SWC.

In this hypothetical case study spatial variability of infiltration produces differences of about 22.8 % in application efficiency and 22.60 % in distribution uniformity of the low quarter for the different inflow locations. The performance of the case study with uniform infiltration (UNI) was better than the best case with spatially varied infiltration.

Indian Basins

In the first field experiment (WALBAS-1) a narrow basin is used to test the model in quasi-one-dimensional conditions. The basin was 75.0 m long by 10 m wide, with an area of 750 sq. m. Water flowing in this field

experiment was largely one-dimensional. Two dual ring infiltrometers were used to estimate the infiltration parameters. The resulting infiltration parameters were $a = 0.00923 \text{ m/min}^b$, $b = 0.386$ and $c = 0.000078 \text{ m/min}$. A value of 0.1 was estimated for Manning's 'n'. The field was irrigated with a constant discharge of $0.147 \text{ m}^3/\text{sec}$ from one of sides. The inflow was cut-off after 65 min. The field test procedure consisted of observations of the advance and recession times at every 5 m along both of the sides of basin by the authors.

In order to test the two-dimensional predictive capability of the model, the authors conducted the second field experiment (WALBAS-2). The experiment was performed in a basin 39.0 m long by 30.0 m wide with an area of 1170 sq. m. The infiltration parameters were computed as $a = 0.00438 \text{ m/min}^b$, $b = 0.412$ and $c = 0.000087 \text{ m/min}$. A value of 0.04 was estimated for the Manning's 'n'. The field was irrigated from a corner with a constant discharge of $0.019 \text{ m}^3/\text{sec}$ and the inflow was cut-off after 35.0 min. Details of these experiments are presented elsewhere (Dholakia 1998).

BASIIT is used for simulating the flow in study basins. Fig. 14 presents the comparison of observed and simulated advance and recession trajectories for basin WALBAS-1. Fig. 15 presents the field and simulated front configurations at 5 min, 10 min, 15 min, 20 min, 25 min and 30 min for basin WALBAS-2. The simulated results match closely with the field observed values.

CLOSURE

The paper presents a computational model for simulation of basin irrigation events. The boundary conditions and stability criteria are also discussed. The results of the models are verified using the observed advance and recession times for basin irrigation events. A good agreement of the results is observed. The model also demonstrates additional features like, considering fan inflow as one of the inflow boundary conditions, spatial variability in infiltration, simulation of high spots and its application to the Indian basins.

Table 1: Comparison of Characteristic times for data of Playan et al.(1994)

EXPERIMENT	TIME OF ADVANCE		TIME OF RECESSION	
	MINUTES	ERROR(%)	MINUTES	ERROR (%)
Field Experiment I				
FIELD DATA	670	-	1815	-
B2D	633	5.50	1822	0.40
SIRMOD	646	3.60	1736	4.40
BASIIT	643	4.00	1830	0.80
Field Experiment II				
FIELD DATA	570	-	1020	-
B2D	525	7.90	900	11.80
SIRMOD	470	17.50	863	15.40
BASIIT	523	8.0	1012	0.78

Table 2 : Results of numerical test for fan inflow

ROWS & COLUMNS	FAN : TWO - DIMENSIONAL				
	NODES	CPU TIME (MIN)	ADVANCE TIME (T_L) (MIN)	RECESSION TIME (T_R) (MIN)	MASS BALANCE ERROR (%)
11 X 11	121	0.153	19.37	123.159	0.683
16 X 16	256	0.710	20.21	124.200	0.592
21 X 21	441	1.940	21.19	124.700	0.562
26 X 26	676	3.940	22.01	125.100	0.456

Table 3 : Simulation results for cases SWC, SEC, NWC, NEC, UNI

CASE	T_l Min	T_r Min	z_r m	E_a %	E_r %	D_u %
SWC	106.540	178.600	0.0414	69.10	97.52	70.75
SEC	107.542	177.500	0.0326	53.30	97.28	54.79
NWC	102.292	180.200	0.0403	67.17	98.60	68.12
NEC	112.347	174.600	0.0333	55.50	98.97	56.08
UNI	097.329	159.400	0.0420	70.00	99.07	70.66

REFERENCES

1. Akanbi, A.A., and Katopodes, N.D. (1988). "Model for flood propagation on initially dry land." *J. Hydr. Engrg.*, ASCE, 114(7), P689-706.
2. Casulli, V. (1990). "Semi-implicit finite difference methods for the two-dimensional shallow water equations." *J. Comput. Physics*, 86, P56-74.
3. Chaudhry, M.H. (1993). "Open-channel flow" Prentice-Hall, inc., Engle Cliffs, N.J., U.S.A.
4. Dholakia, M. (1998). "Simulation, Parameteric study, Sensitivity analysis, Parameter estimation, Field studies, Design and Hydrodynamic stability of surface irrigation systems." Ph.D. thesis, I.I.T. Bombay, Mumbai, India.
5. Katopodes, N.D., and Strelkoff, T. (1978) "Computing two-dimensional dam break flood waves." *J. Hydr., Engr., Div.*, ASCE, 104(9), P1269-1288.
6. Katopodes, N.D. (1980). "Finite element model for open channel flow near critical conditions." Finite elements in water resources III, S.Y. Wang, Ed., University of Mississippi Press, University, Miss, P 5.37-7.46.
7. Katopodes, N.D., and Wu, C. (1986). "Explicit computation of discontinuous channel flow." *J. Hydr., Engr., Div.*, ASCE, 112(6), P456-475.
8. Mader, C.L. (1988). "Numerical modelling of water waves." University of California Press, Berkley, Calif.
9. Playan, E., Walker, W.R., and Merkley, G.P. (1994). "Two-dimensional simulation of basin irrigation. I & II : applications." *J. Irrig. drain. Engrg.* ASCE, 120(5), P 857-870.
10. Reid, R. O., and Bodine, B. R. (1968). "Numerical model for storm surges in Galveston bay." *J. Waterways and Harbours Div.*, ASCE, 94(1), P 33-57.
11. Roache, P.J., 1972. *Computational fluid dynamics*. Hermosa Publishers, Albuquerque, N.M.
12. Singh, V., and Murthy, B.S. (1998). "Basin Irrigation Simulation." *J. Irrig. & Drain. Engrg.* ASCE.
13. Walters, R.A., and Cheng, R.T. (1979). "A two-dimensional hydrodynamic model for tidal estuary." *Advances in Water Resources*, 1979(2), P 177-184.
14. Xanthopoulos, T., and Koutitas, C. (1976). "Numerical simulation of a two-dimensional flood wave propagation due to dam failure." *J. Hydr. Res.*, 14(4), P 321-331.

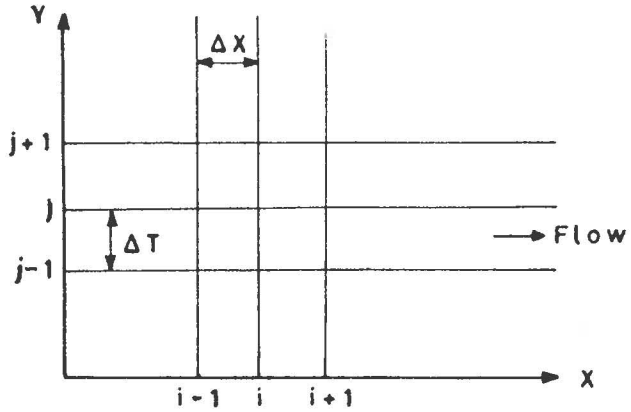


Fig. 1 : Finite Difference Discretisation of the Domain

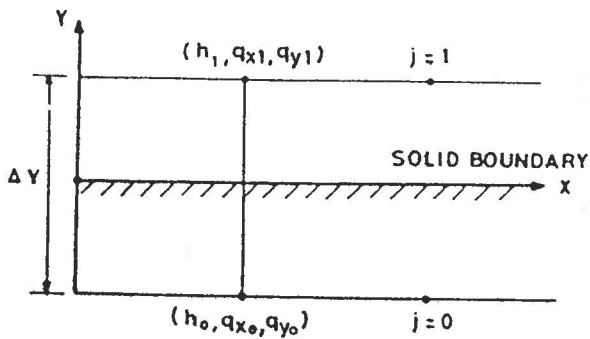


Fig. 2 : Reflection Boundary

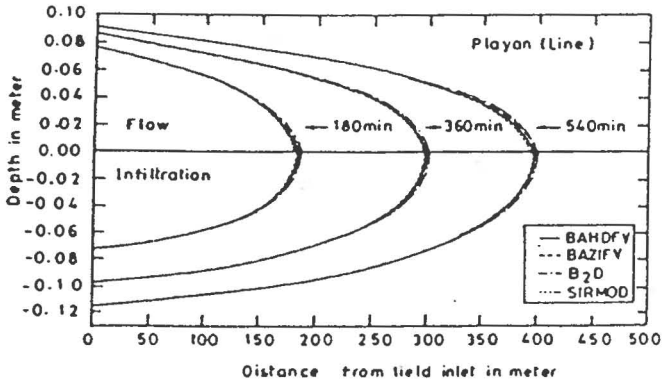


Fig. 3 : Overland and infiltration profiles (Line Inflow)

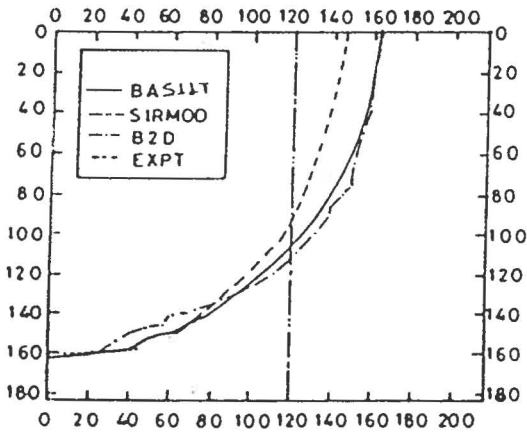


Fig. 4 : Front Configuration at 3 Hour for Level Basin (Corner Inflow)

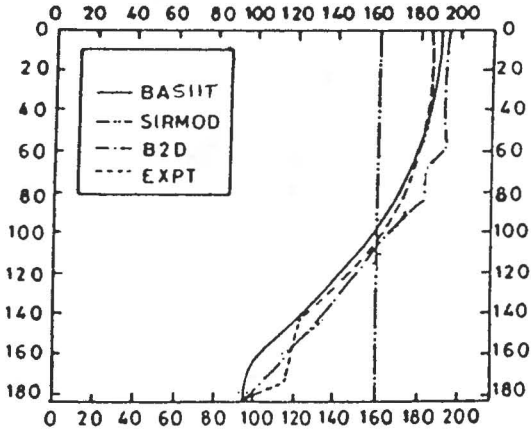


Fig. 5 : Front Configuration at 5 Hour for Level Basin (Corner Inflow)

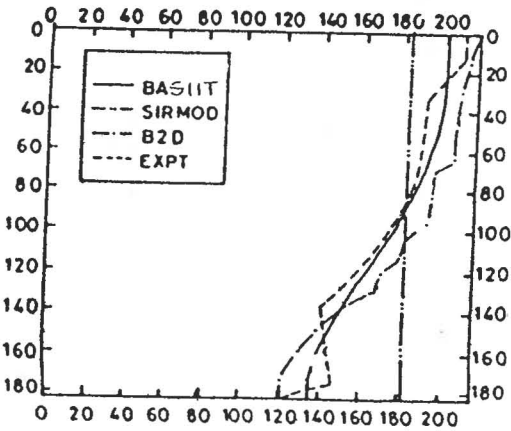


Fig. 6 : Front Configuration at 6 Hour for Level Basin (Corner Inflow)

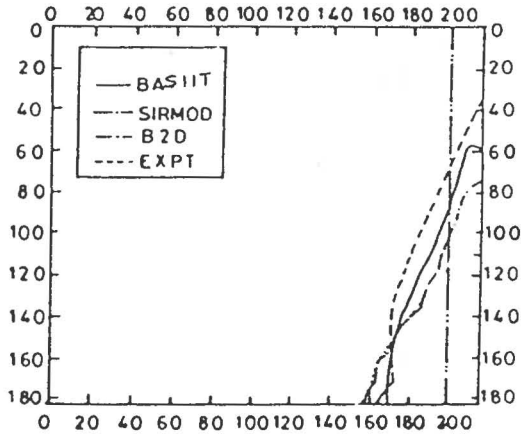


Fig. 7 : Front Configuration at 7 Hour for Level Basin (Corner Inflow)

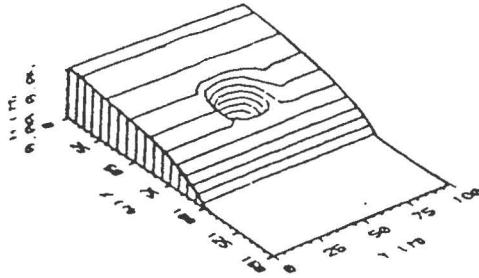


Fig. 8 : Flow Past High Spot at 30 Min (Line Inflow)

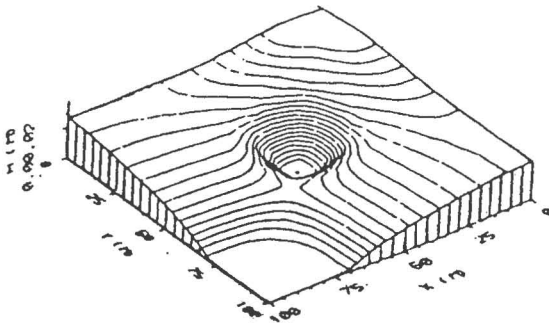


Fig. 9 : Flow Past High Spot at 40 Min (Corner Inflow)

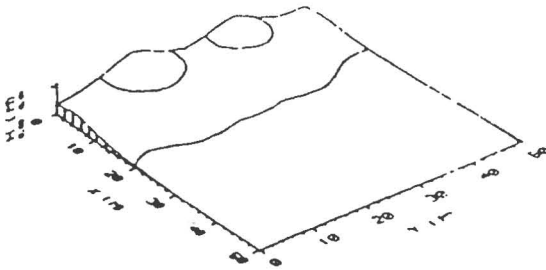


Fig. 10 : Overland Profile at 15 Min (Fan Inflow)

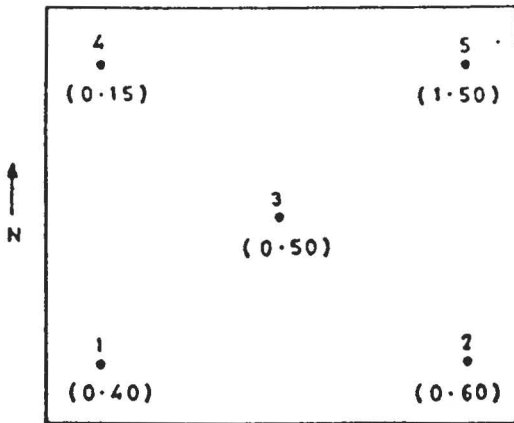


Fig. 11 : Location of Infiltration test sites

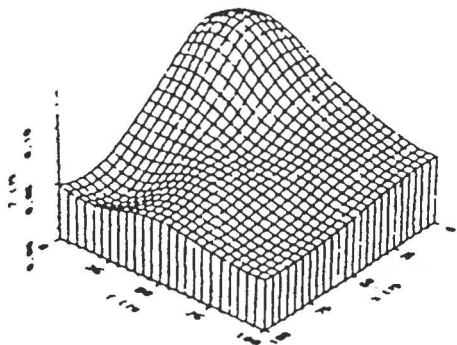


Fig. 12 : 3D map of Infiltration Depths for NEC

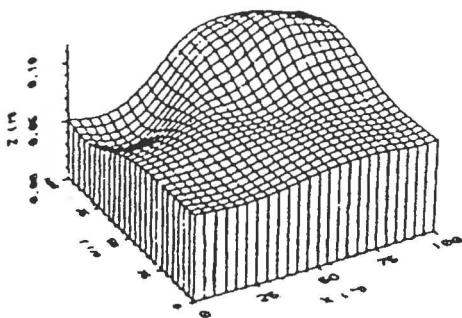


Fig. 13 : 3D map of Infiltration Depths for SWC

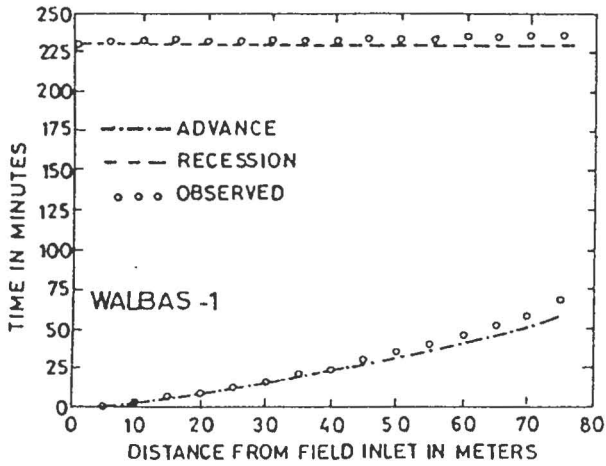


Fig. 14 : Observed and Simulated Advance and Recession Trajectories (WALBAS-1)

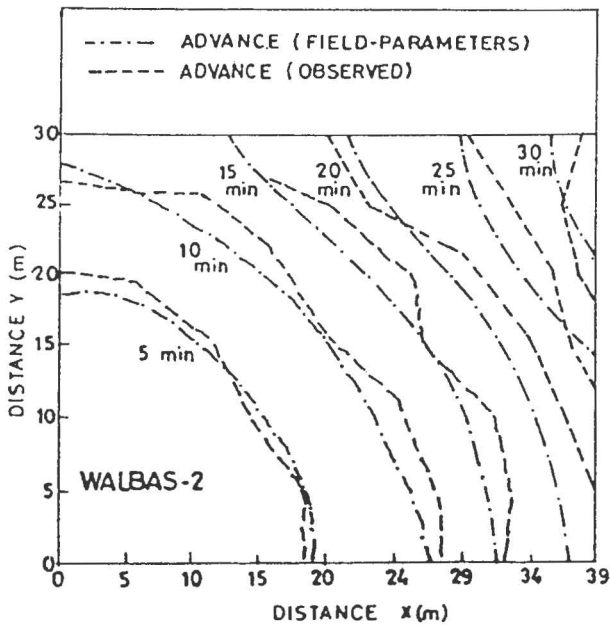


Fig. 15 : Observed and Simulated Advance and Recession Trajectories (WALBAS-2)